



**HAL**  
open science

# Synthesis, Characterization, and Electrochemical Applications of Chiral Imprinted Mesoporous Ni Surfaces

Sunpet Assavapanumat, Marisa Ketkaew, Alexander Kuhn, Chularat Wattanakit

► **To cite this version:**

Sunpet Assavapanumat, Marisa Ketkaew, Alexander Kuhn, Chularat Wattanakit. Synthesis, Characterization, and Electrochemical Applications of Chiral Imprinted Mesoporous Ni Surfaces. *Journal of the American Chemical Society*, 2019, 141 (47), pp.18870-18876. 10.1021/jacs.9b10507. hal-02509914

**HAL Id: hal-02509914**

**<https://hal.science/hal-02509914>**

Submitted on 17 Mar 2020

**HAL** is a multi-disciplinary open access archive for the deposit and dissemination of scientific research documents, whether they are published or not. The documents may come from teaching and research institutions in France or abroad, or from public or private research centers.

L'archive ouverte pluridisciplinaire **HAL**, est destinée au dépôt et à la diffusion de documents scientifiques de niveau recherche, publiés ou non, émanant des établissements d'enseignement et de recherche français ou étrangers, des laboratoires publics ou privés.

# Synthesis, Characterization and Electrochemical Applications of Chiral Imprinted Mesoporous Ni Surfaces

Sunpet Assavapanumat,<sup>†,‡</sup> Marisa Ketkaew,<sup>†,‡</sup> Alexander Kuhn<sup>\*,‡</sup> and Chularat Wattanakit<sup>\*,†</sup>

<sup>†</sup> School of Molecular Science and Engineering, School of Energy Science and Engineering and Nanocatalysts and Nanomaterials for Sustainable Energy and Environment Research Network of NANOTEC, Vidyasirimedhi Institute of Science and Technology, Rayong, 21210, Thailand.

<sup>‡</sup> University of Bordeaux, CNRS, UMR 5255, Bordeaux INP, Site ENSCBP, 16 avenue Pey Berland, 33607, Pessac, France.

**ABSTRACT:** The enantioselective synthesis of chiral compounds is of crucial importance for a wide range of potential applications, especially in cosmetic and pharmaceutical industries. Recently, chiral imprinted mesoporous platinum films, produced by the electrodeposition of the metal, in the simultaneous presence of a lyotropic liquid crystalline phase of non-ionic surfactants as mesoporegens and chiral templates, have been applied as electrocatalysts and selective stationary phases for the asymmetric synthesis and separation of chiral compounds, respectively. However, platinum is an expensive metal and therefore it is mandatory to explore the possibility to apply this concept also to other metals. In this contribution, we propose mesoporous chiral imprinted nickel as an alternative cheap and earth-abundant metal. The designed surface layers not only demonstrate electrochemical discrimination between two enantiomers, but most importantly, also allow stereospecific electroreduction of a prochiral compound, with very significant enantioselectivity of up to 80% ee. These results open up very promising perspectives for the development of low cost non-noble metal matrices for the synthesis of chiral compounds.

## INTRODUCTION

Engineering of chiral surfaces has been one of the most attractive topics in the chemical community because they can be used to generate enantiomerically pure compounds (EPC).<sup>1</sup> Although, there are several methods that have been proposed to obtain a single enantiomer,<sup>2</sup> asymmetric synthesis is one of the most promising approaches.<sup>3</sup> Until now, asymmetric catalysis, based on the use of chiral catalysts, has been extensively illustrated with chiral coordination complexes,<sup>4</sup> molecular imprinted polymers,<sup>5</sup> and biocatalysts.<sup>6</sup> Over the past decades, homogeneous catalysts have played an important role in asymmetric synthesis due to an efficient up-scaling of production.<sup>7</sup> However, much effort is required to recover the catalyst from the reaction mixtures.<sup>8</sup> Often, a highly efficient enantioselective synthesis is based on the use of biocatalysts, which provide a specific asymmetric environment for the generation of chiral molecules under mild conditions.<sup>6,9</sup> Nevertheless, low efficiency, poor stability under operating conditions and a narrow substrate spectrum of biocatalysts are considered as key limitations.<sup>10</sup>

To mimic chiral biocatalytic platforms, many different approaches, for example based on molecular imprinting,<sup>11</sup> molecular grafting,<sup>12</sup> as well as organometallic<sup>13</sup> and coordination chemistry<sup>4,14</sup> have been explored. Among them, the molecular imprinting approach has been extensively developed, because it is easy to generate a large variety of chiral cavities.<sup>15</sup> Over the past decade, the chiral molecular imprinting approach has been mostly focused on imprinted polymers (MIP), which can show high affinity and selectivity in chiral recognition.<sup>16</sup> However, their highly flexible structure and the difficulty to retain the chiral information after template removal are main drawbacks.<sup>17</sup> Therefore, other materials have also been explored in this context such as silica,<sup>18</sup> silica/polymer hybrid materials<sup>19</sup> or metals.<sup>20</sup> In the latter case the recognition efficiency can be greatly enhanced when the

chiral information is integrated in a mesoporous matrix.<sup>2a,2e,3c,3d,21</sup> This has been illustrated with chiral-encoded mesoporous Pt obtained by electrodeposition of the metal in the simultaneous presence of a lyotropic crystalline phase and chiral compounds. The resulting materials have been successfully used for various applications ranging from enantioselective recognition,<sup>2a,2e</sup> asymmetric synthesis of chiral compounds,<sup>3c,3d</sup> and chiral separation.<sup>2h</sup>

Although these structures have shown very interesting features from an academic point of view, a major drawback with respect to practical applications is the fact the platinum is an expensive precious metal with a deleterious environmental impact.<sup>22</sup> In order to open up realistic application perspectives, imprinting chiral information in earth-abundant first-row transition metals, such as for example nickel, would be an extremely important achievement in terms of cost and sustainability.<sup>23</sup> In addition, nickel is also an interesting alternative metal in terms of chemical features, because it shows high activity in several electrocatalytic reactions, such as hydrogen production or enantioselective hydrogenation,<sup>24</sup> oxygen reduction<sup>25</sup> and especially electroreduction of organic molecules.<sup>26</sup>

It is well-known that the incorporation of mesoporous features into bulk materials leads to outstanding properties, especially a very high active surface area.<sup>27</sup> To design such materials, there are many different approaches, including both chemical and electrochemical methods.<sup>28</sup> Over the past decade, mesoporous Ni has been successfully obtained via electrodeposition in the presence of various types and concentrations of surfactants as mesoporegens.<sup>29</sup> The resulting porous electrodes show a very high surface area, although they are only present as thin layers deposited with a low amount of charge.<sup>30</sup> Many literature reports are dedicated to the (electro)catalytic applications of such high surface area nickel, but molecular imprinting of chiral information in such a matrix has not yet been demonstrated.

In this contribution, we report the production of chiral mesoporous Ni surfaces by electrodeposition of Ni in the simultaneous presence of non-ionic surfactant (Brij C10) and a chiral compound (phenylethanol, PE). The chiral character of the generated surfaces is revealed by discriminatory electrooxidation of the two PE enantiomers. In addition, and most importantly, the designed material is used for the enantioselective electroreduction of acetophenone as a prochiral model compound to produce the initially imprinted PE enantiomer with a high excess.

## RESULTS AND DISCUSSION

### Electrodeposition of chiral imprinted mesoporous Ni films

Chiral encoded mesoporous Ni has been successfully prepared by electrodeposition from Ni acetate in the presence of a self-assembled lyotropic liquid crystalline phase and the desired enantiomer as shown in Scheme 1 (see Supporting Information for a detailed description). Scheme 1a represents the molecular structure of the chiral templates, (R)-PE and (S)-PE, which are the target molecules for the electroreduction of acetophenone. Due to the hydrophilic interaction (H-bonding) between the hydroxyl group of the chiral molecules and the head groups of the non-ionic surfactant, Brij C10, the chiral compounds are located preferentially at the outer surface of the surfactant columns constituting the self-assembled hexagonal structure ( $H_1$ ) of the lyotropic liquid crystal phase (Scheme 1b). When metallic nickel is grown around this soft template (Scheme 1c), mesoporous channels and chiral imprinted cavities are obtained after removal of the template (Scheme 1d).

Microscopic characterisation of a Ni film, obtained by using a charge density of  $4 \text{ C cm}^{-2}$  for the electrodeposition, reveals a smooth surface with uniform thickness over the entire area (Figures 1a and 1b). Obviously, the thickness of the mesoporous Ni films can be easily tuned by changing the charge density used for the electrodeposition (Figure S1). For example, the thickness resulting from a deposition charge density of 1, 2 and  $4 \text{ C cm}^{-2}$  is 1.0, 1.8 and  $4.0 \mu\text{m}$  respectively. TEM investigation of a film generated with a charge density of  $100 \text{ mC cm}^{-2}$ , reveals a uniform mesopore size distribution in the range of  $2.33 \pm 0.22 \text{ nm}$  (Figure 1c), which is in agreement with the expected pore size for this type of surfactant.

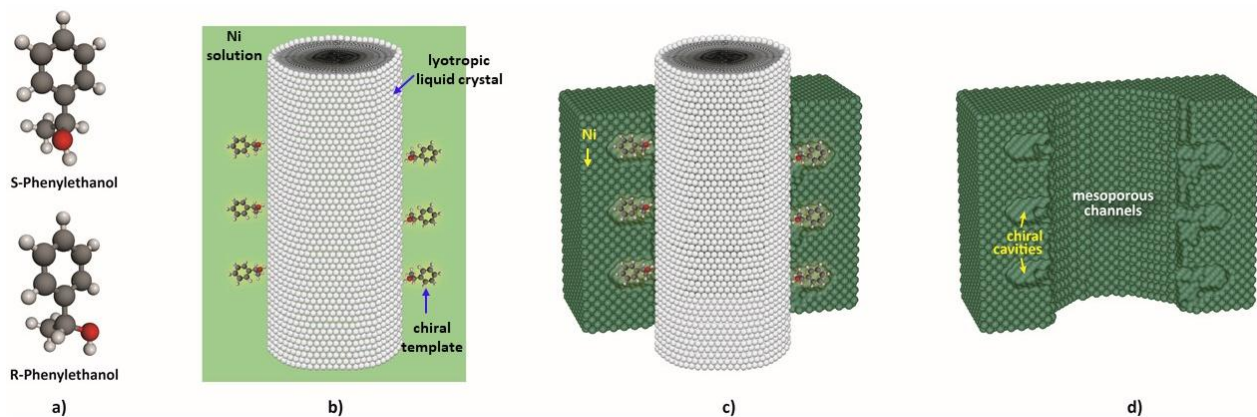
In addition, to confirm the high active surface area of the film, the electrochemical properties in 1 M KOH were monitored by cyclic voltammetry (CV). Well-defined oxidation and reduction peaks are observed in the potential range from 250 to 350 mV and

100 to 250 mV vs Ag/AgCl, respectively (Figure 1d). The current density of the oxide-layer formation correlates with the active surface area of the Ni electrodes.<sup>31</sup> The relative roughness factors of the prepared electrodes obtained with various deposition charge densities of 1, 2 and  $4 \text{ C cm}^{-2}$  are 28.3, 61 and 114.2, respectively, indicating a linear correlation (Figure S2). The relationship between the relative roughness factor and the thickness of the electrodes measured by SEM (Figure S1) leads as well to a linear dependence (Figure S2).

### Enantioselective recognition of chiral compounds at chiral imprinted mesoporous Ni surfaces

In order to illustrate the enantioselective properties of the chiral encoded Ni layers, differential pulse voltammetry (DPV) was used for the enantioselective electrooxidation PE. Compared to cyclic voltammetry this allows decreasing the impact of capacitive current, which is very high for such mesoporous layers, and therefore a more pronounced discrimination in terms of faradaic current becomes possible. Prior to studying the enantioselective recognition properties, the complete removal of chiral template was confirmed by two independent methods: (i) examining the amount of removed chiral template as a function of rinsing time by UV-VIS spectroscopy; (ii) monitoring the electrooxidation current of eventually remaining chiral compound by DPV. As shown in Figure S3, a series of UV-Vis spectra of the different washing solutions was recorded to confirm the progressive template removal when rinsing for 36 h. In addition, to further confirm the removal of chiral molecules, a DPV in supporting electrolyte (50 mM HCl) of chiral imprinted mesoporous Ni after rinsing for 36 h was measured in the potential range from 400 to 530 mV vs. Ag/AgCl as shown in Figure S4. Indeed, no oxidation peak of PE was observed from 410 to 530 mV (oxidation region of PE) for the imprinted electrode after washing. To further confirm the absence of parasitic phenomena, the DPV signals for both enantiomers on a non-imprinted mesoporous nickel electrode were compared. As expected, identical DPV current densities for the electrooxidation of (S)-PE (red) and (R)-PE (blue) were observed, confirming the absence of chiral information (Figure 2a). In strong contrast, the chiral imprinted mesoporous Ni allows discriminating the two enantiomers (Figures 2b and 2c). Chiral mesoporous Ni imprinted with (S)-PE exhibits a more pronounced signal for (S)-PE (red) with respect to (R)-PE (blue), whereas the one imprinted with (R)-PE shows a significantly higher signal for (R)-PE (blue) compared to (S)-PE (red). These observations clearly confirm the presence of chiral information in these metal layers, even after removal of the chiral templates. However, due to the easy oxidation of nickel, it is difficult to maintain the chiral imprints when exposing the electrodes to positive potentials.<sup>32</sup>

**Scheme 1.** Illustration of the formation of a chiral imprinted mesoporous Ni film in the simultaneous presence of the lyotropic liquid crys-



talline phase ( $H_1$ ) and chiral compounds: a) the molecular structure of (S) and (R)-PE; b) a self-assembled column of the lyotropic liquid

crystalline phase in the presence of chiral molecules and Ni salt; c) Ni deposition in the presence of the two types of template; d) the chiral imprinted mesoporous Ni obtained after the dissolution of the templates

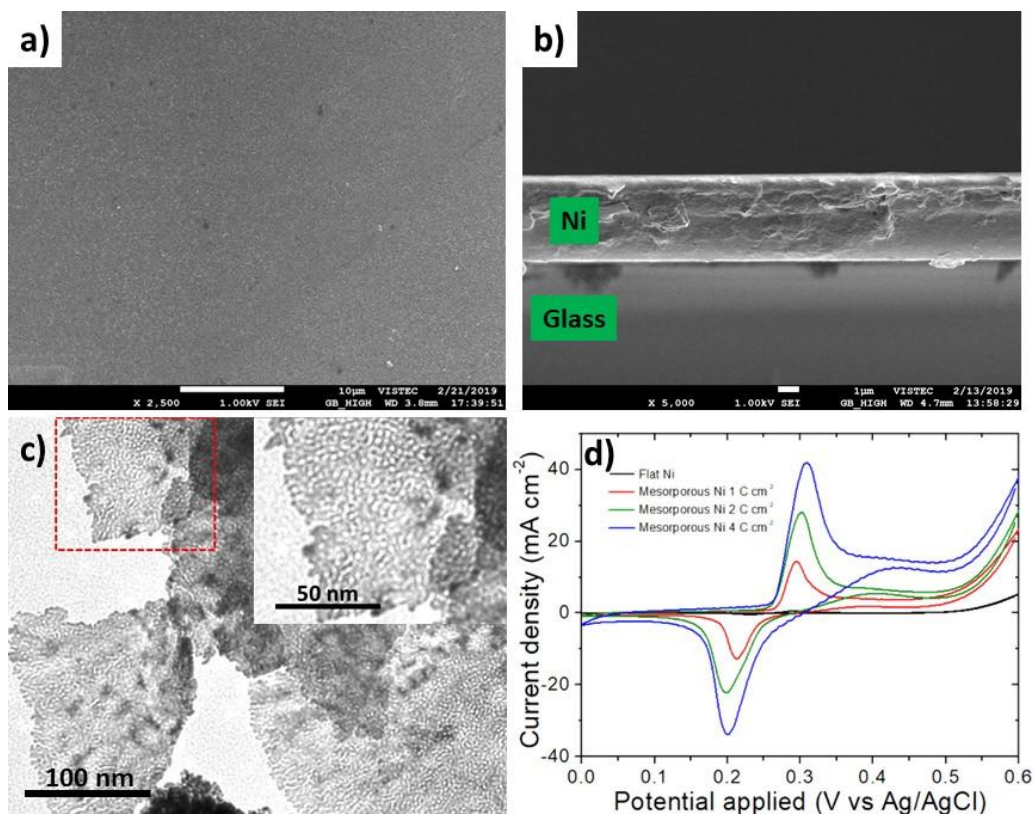


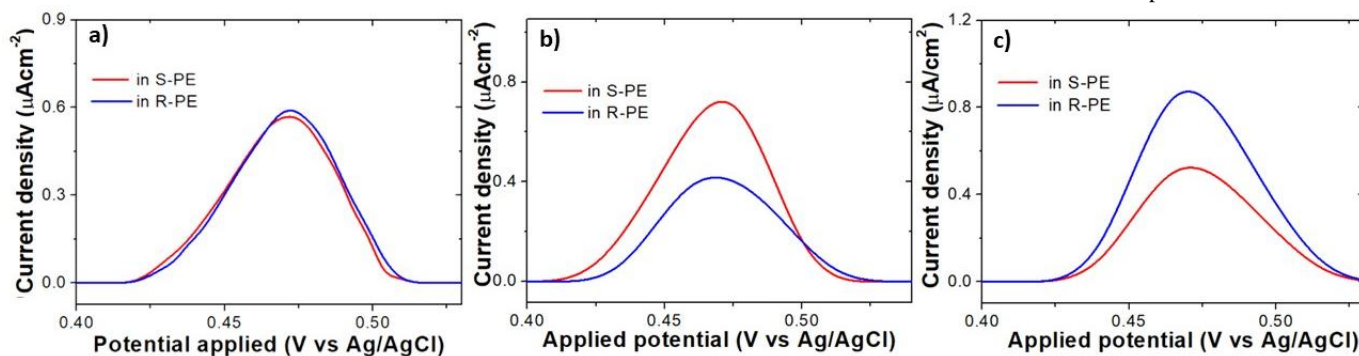
**Figure 1.** Characterization of chiral imprinted mesoporous Ni films: a) and b) SEM images (top view and cross section) of mesoporous nickel imprinted with S-PE obtained with a deposition charge density of 4 C cm<sup>-2</sup> (scale bar 10 μm (top view) and 1 μm (cross section)); c) TEM image of a mesoporous Ni film obtained with a charge density of 100 mC cm<sup>-2</sup> and d) cyclic voltammograms of chiral-imprinted mesoporous Ni electrodes prepared with various charge densities compared to flat Ni in 1 M KOH at a scan rate of 100 mVs<sup>-1</sup>.

### Asymmetric synthesis of chiral compounds at chiral imprinted mesoporous Ni surfaces

In previous reports, the use of chiral encoded noble metal surfaces for the enantioselective electrosynthesis of chiral compounds from a prochiral precursor molecule has been described.<sup>3c,3d</sup> It was found that by fine-tuning the electrosynthesis potential, as well as applying potential pulses with varying duration, a highly selective production of chiral compounds is possible.<sup>3d</sup> In this contribution, we describe for the first time the possibility to use this concept also for non-noble metals. This is not an easy task as such metals

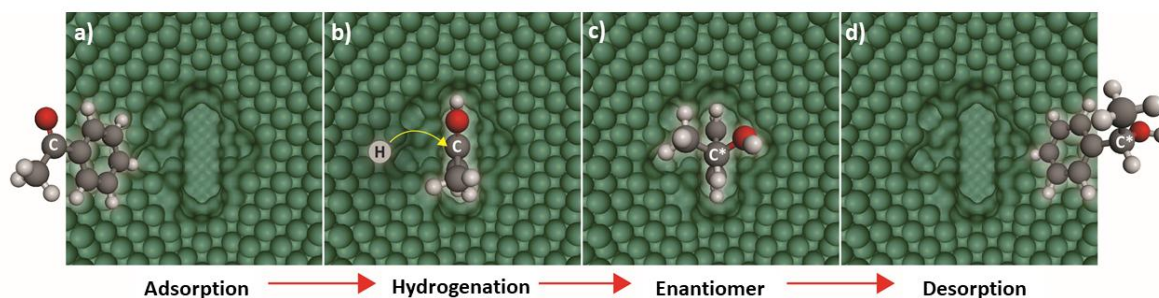
are much more reactive and might lose very quickly the chiral information by surface oxidation.

The electrochemical reduction of acetophenone to PE has been chosen as a model reaction. To achieve highly enantioselective synthesis, acetophenone needs first to adsorb in the chiral metal matrix (Scheme 2a). Subsequently, its carbonyl group (C=O) is reduced in the chiral cavities (Scheme 2b). Due to the asymmetric local environment, a chiral product, which fits the spatial configuration of the encoded structure, is selectively produced during this hydrogenation step (Scheme 2b and 2c). Finally, the chiral product is desorbed from the reaction site as represented in Scheme



2d.

**Figure 2.** Differential pulse voltammograms (DPV) of the electrooxidation of (R)-PE (blue) and (S)-PE (red) in 50 mM HCl as a supporting electrolyte with different electrodes: a) flat Ni electrode, b) chiral mesoporous Ni electrode imprinted with (S)-PE, and (c) chiral mesoporous Ni electrode imprinted with (R)-PE.



**Scheme 2.** Enantioselective synthesis steps of phenylethanol ((R)-PE or (S)-PE) during the electroreduction of acetophenone: a) adsorption of the prochiral molecule, acetophenone, in the chiral cavity; (b) hydrogenation of acetophenone inside the chiral cavity; (c) formation of PE inside the corresponding chiral cavity; (d) desorption of the PE enantiomer.

An optimized potential of  $-550$  mV vs. Ag/AgCl was applied for the synthesis because the reduction of the prochiral functional C=O group of acetophenone molecules starts around this potential. More negative potentials might induce an interference with proton reduction that may generate hydrogen bubbles, eventually destroying the mesoporous structure. Thus, the applied potential should be in the range from  $-450$  to  $-550$  mV vs. Ag/AgCl in order to allow a selective electroreduction at the C=O functional group (Figure S5).

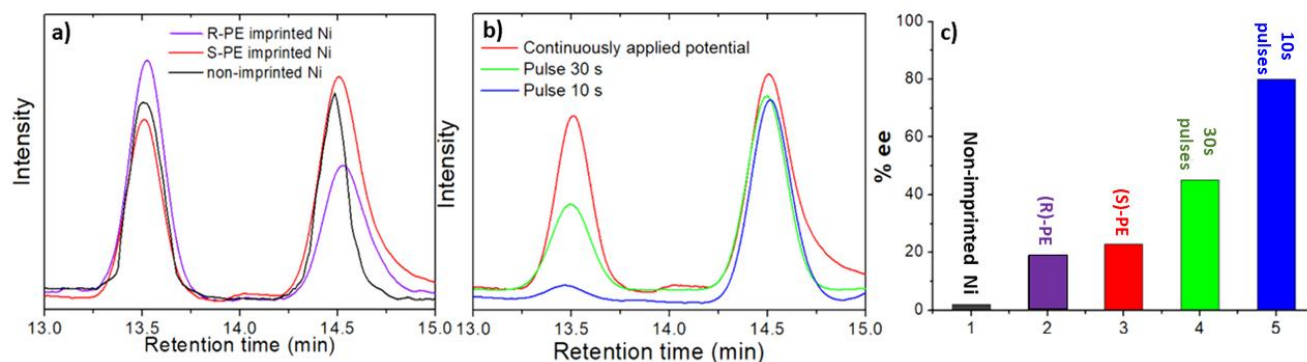
As illustrated in Figure 3, the degree of enantioselectivity was determined by high-performance liquid chromatography (HPLC). Figure S6 shows the chromatograms of prochiral acetophenone, (R)-PE, and (S)-PE, with retention times of 10.1 (black), 13.5 (red), and 14.5 (blue) min, respectively. In a control experiment, using non-imprinted mesoporous Ni as a working electrode, a very low % enantiomeric excess (% ee) of 1.9% is observed. Considering the error bar or the s.e.m. of the % ee value ( $\pm 3.61$  %), calculated by equation 2 in the supporting information, this indicates that there is no enantioselectivity in this case. However, when using chiral mesoporous Ni imprinted with (S)-PE, an % ee of 23 % was obtained after applying a constant potential for 12h. The corresponding control experiment, carried out with an R-(PE) imprinted electrode, resulted in an % ee of -19 %. These first results are a promising proof-of-principle that chiral information can be retained by mesoporous nickel, even though the selectivity is rather moderate.

As previously reported,<sup>3d</sup> the concept of pulsed electrosynthesis with chiral encoded noble metal surfaces allows one to signifi-

cantly improve the enantioselectivity due to a partial suppression of the competing reactions at the non-imprinted metal located at the external electrode surface. In order to improve the % ee in the case of nickel surfaces, a potential of  $-550$  mV vs. Ag/AgCl was applied with different pulse durations. For a pulse duration of 30 s the % ee is significantly improved from 23 % to 45 % with respect to conventional steady-state electroreduction (Figure 3b). Even more pronounced enantioselectivity can be obtained when using a shorter pulse duration of 10 s. In this case, the % ee eventually reaches 80 % as shown in Figure 3c. From a theoretical point of view, this can be understood by the fact that a decrease of pulse duration favors the reaction in the enantioselective mesopores due to the high internal surface area compared to the rather small outer non-imprinted surface.<sup>3d</sup> Short potential pulses, alternating with relaxation periods enable the produced enantiomer to evacuate the porous metal and allow diffusion of fresh prochiral precursor into the mesoporous matrix.

Compared to the previously studied platinum, nickel, as a non-noble metal, has a much lower mechanical and chemical stability.<sup>33</sup> Therefore, it is crucial to investigate also the stability of the imprinted chiral information. When chiral imprinted mesoporous Ni electrodes are immersed into the supporting solution without any applied potential under continuous stirring in nitrogen atmosphere, the mesoporous Ni layer gets nevertheless oxidized and is completely removed after 1 day, as illustrated in Figure S7. However, when a negative potential is applied, the mesoporous Ni layer is able to tolerate the synthesis conditions without significant degradation, due to the presence of a cathodic protection.<sup>34</sup>

**Figure 3.** Enantioselective electrosynthesis with chiral imprinted Ni electrodes: a) and b) HPLC chromatograms of electrosynthesis prod-



ucts obtained with imprinted electrodes in 10 mM acetophenone and 1 M  $\text{NH}_4\text{Cl}$  at a constant potential (a) or pulsed potential (b) mode for  $E = -0.55$  V vs Ag/AgCl. The peak retention times of 13.5 and 14.5 min correspond to (R)-PE and (S)-PE, respectively. c) Histogram summarizing the enantiomeric excess (%ee) of the different experiments. Colour codes illustrate the different condition of electrosyn-

thesis: non-imprinted Ni (black); (R)-PE imprinted Ni (purple) and (S)-PE imprinted Ni with continuously applied potential (red); (S)-PE imprinted Ni with 30s potential pulses (green) and (S)-PE imprinted Ni with 10s potential pulses (blue).

## CONCLUSIONS

Chiral-encoded mesoporous nickel has been successfully prepared by electrodeposition from Ni acetate in the simultaneous presence of a lyotropic liquid crystal phase of non-ionic surfactant, Brij C10, and a chiral compound, phenylethanol. Characterization of the physical and electrochemical properties of the prepared films reveals that the active surface area is enhanced by two orders of magnitude compared to flat Ni. This allows a significant discrimination between (R)-PE and (S)-PE enantiomers, confirmed by DPV. Most importantly, the designed materials can be used for the enantioselective electroreduction of a prochiral compound, acetophenone, leading to preferential formation of one or the other phenylethanol enantiomer. The % ee can be greatly improved when using the concept of pulsed electrosynthesis. By fine-tuning the pulse duration, an optimized %ee of up to 80 % can be achieved, which is extremely high for such a non-noble heterogeneous catalytic system. Therefore this work is a crucial extension of the concept of chiral imprinting to non-noble metals and offers an interesting perspective for the development of designer materials for the chiral synthesis of high-added-value chemicals. Many pharmaceutical compounds actually contain chiral alcohol groups and it should be quite straight forward to extend the presented proof-of-principle experiments to such molecules. The chiral encoded layers could then replace or complement other approaches, for example based on the use of enzymes, with the chiral metal cavities playing the role of a biomimetic equivalent of the enzymatically active reaction site, allowing the stereoselective synthesis of chiral alcohols as important pharmaceutical products or intermediates.<sup>35</sup>

## ASSOCIATED CONTENT

### Supporting Information.

The Supporting Information is available free of charge on the ACS Publication website at DOI:.

## AUTHOR INFORMATION

### Corresponding Author

\*[chularat.w@vistec.ac.th](mailto:chularat.w@vistec.ac.th)

\*[kuhn@enscbp.fr](mailto:kuhn@enscbp.fr)

## ACKNOWLEDGMENT

We would like to thank Sopon Butcha for TEM sample preparation and the grant from Vidyasirimedhi Institute of Science and Technology (VISTEC). This work was supported by the bilateral PICS program of CNRS. Chu. W. thanks the Thailand Research Fund (TRF) (MRG6180099), the Office of Higher Education Commission (OHEC) and TTSF research project supported by Thailand Toray Science Foundation. In addition, this work has been partially supported by the National Nanotechnology Center (NANOTEC), NSTDA, Ministry of Science and Technology, Thailand, through its program of Research Network NANOTEC (RNN). S.A. is grateful to Campus France, the France Embassy in Thailand and VISTEC for a Ph.D. cotutelle scholarship. The project has also been partially funded by the European Research Council (ERC) under the European Union's Horizon 2020 research and innovation program (grant agreement n° 741251, ERC Advanced grant ELECTRA).

## REFERENCES

- (1) (a) Mitchell, A. G. Racemic Drug: Racemic Mixture, Racemic Compound, or Pseudoracemate? *J. Pharm. Pharmacol. Sci.* **1998**, *1*, 8-12. (b) McConathy, J.; Owens, M. J. Stereochemistry in Drug Action. *Prim. Care Companion. J. Clin. Psychiatry.* **2003**, *5*, 70-73. (c) Chhabra, N.; Aseri, M. L.; Padmanabhan, D. A Review of Drug Isomerism and Its Significance. *Int. J. Appl. Basic. Med. Res.* **2013**, *3*, 16-18. (d) Sannicolò, F.; Arnaboldi, S.; Benincori, T.; Bonometti, V.; Cirilli, R.; Dunsch, L.; Kutner, W.; Longhi, G.; Mussini, P. R. Panigati, M.; Pierini, M.; Rizzo, S. Potential-Driven Chirality Manifestations and Impressive Enantioselectivity by Inherently Chiral Electroactive Organic Films. *Angew. Chem. Int. Ed.* **2014**, *53*, 2623-2627. (e) Attard, G. A. Electrochemical Studies of Enantioselectivity at Chiral Metal Surfaces. *J. Phys. Chem. B* **2001**, *105*, 3158-3167.
- (2) (a) Wattanakit, C.; Côme, Y. B. S.; Lapeyre, V.; Bopp, P. A.; Heim, M.; Yadnum, S.; Nokbin, S.; Warakulwit, C.; Limtrakul, J.; Kuhn, A. Enantioselective Recognition at Mesoporous Chiral Metal Surfaces. *Nat. Comm.* **2014**, *5*, 3325. (b) Pandey, I.; Kant, R. Electrochemical Impedance Based Chiral Analysis of Anti-Ascorbic Drug: L-Ascorbic acid and D-Ascorbic acid using C-Dots Decorated Conductive Polymer Nano-Composite Electrode. *Biosens. Bioelectron.* **2016**, *77*, 715-724. (c) Sun, M.; Qu, A.; Hao, C.; Wu, X.; Xu, L.; Xu, C.; Kuang, H. Chiral Upconversion Heterodimers for Quantitative Analysis and Bioimaging of Antibiotic-Resistant Bacteria In Vivo. *Adv. Mater.* **2018**, *30*, 1804241. (d) Pu, C.; Xu, Y.; Liu, Q.; Zhu, A.; Shi, G. Enantiomers of Single Chirality Nanotube as Chiral Recognition Interface for Enhanced Electrochemical Chiral Analysis. *Anal. Chem.* **2019**, *91*, 3015-3020. (e) Yutthalekha, T.; Warakulwit, C.; Limtrakul, J.; Kuhn, A. Enantioselective Recognition of DOPA by Mesoporous Platinum Imprinted with Mandelic Acid. *Electroanal.* **2015**, *27*, 2209-2213. (f) Chen, C.; Shi, H.; Zhao, G. Chiral Recognition and Enantioselective Photoelectrochemical Oxidation toward Amino Acid on Single-Crystalline ZnO. *J. Phys. Chem. C*, **2014**, *118*, 12041-12049. (g) Bruno, R.; Marino, N.; Bartella, L.; Donna, L. D.; Munno, G. D.; Pardo, E.; Armentano, D. Highly Efficient Temperature-Dependent Chiral Separation with a Nucleotide-Based Coordination Polymer. *Chem. Commun.* **2018**, *54*, 6356-6359. (h) Assavapanumat, S.; Yutthalekha, T.; Garrigue, P.; Goudeau, B.; Lapeyre, V.; Perro, A.; Sojic, N.; Wattanakit, C.; Kuhn, A. Potential Induced Fine-Tuning of the Enantioaffinity of Chiral Metal Phases. *Angew. Chem. Int. Ed.* **2019**, *58*, 3471-3475. (i) Anand, D.; Dhoke, G. V.; Gehrman, J.; Garakani, T. M.; Davari, M. D.; Bocola, M.; Zhu, L.; Schwaneberg, U. Chiral Separation of D/L-Arginine with Whole Cells through An Engineered FhuA Nanochannel. *Chem. Commun.* **2019**, *55*, 5431-5434; (j) Ye, X.; Cui, J.; Li, B.; Li, N.; Wang, R.; Yan, Z.; Tan, J.; Zhang, J.; Wan, X. Enantiomer-Selective Magnetization of Conglomerates for Quantitative Chiral Separation. *Nat. Commun.* **2019**, *10*, 1964. (k) Kupai, J.; Rojik, E.; Huszthy, P.; Szekely, G. Role of Chiral and Macroring in Imprinted Polymers with Enantiodiscriminative Power. *ACS Appl. Mater. Interfaces* **2015**, *7*, 9516-9525. (l) Mallat, T.; Orglmeister, E.; Baiker, A. Asymmetric Catalysis at Chiral Metal Surfaces. *Chem. Rev.* **2007**, *107*, 4863-4890.
- (3) (a) Pavlidis, I. V.; Weiß, M. S.; Genz, M.; Spurr, P.; Hanlon, S. P.; Iding, H.; Bornscheuer, U. T. Identification of (S)-Selective Transaminases for The Asymmetric Synthesis of Bulky Chiral Amines, *Nat. Chem.* **2016**, *8*, 1076-1082. (b)

- Simeonov, S. P.; Nunes, J. P. M.; Guerra, K.; Kurteva, V. B.; Afonso, C. A. M. Synthesis of Chiral Cyclopentenones. *Chem. Rev.* **2016**, *116*, 5744-5893. (c) Yuthalekha, T.; Wattanakit, C.; Lapeyre, V.; Nokbin, S.; Warakulwit, C.; Limtrakul, J.; Kuhn, A. Asymmetric Synthesis Using Chiral-Encoded Metal. *Nat. Commun.* **2016**, *7*, 12678. (d) Wattanakit, C.; Yuthalekha, T.; Assavapanumat, S.; Lapeyre, V.; Kuhn, A. Pulsed Electroconversion for Highly Selective Enantiomer Synthesis. *Nat. Commun.* **2017**, *8*, 2087. (e) Xue, Y. P.; Cao, C. H.; Zheng, Y. G. Enzymatic Asymmetric Synthesis of Chiral Amino Acids. *Chem. Soc. Rev.* **2018**, *47*, 1516-1561. (f) Wang, D. W.; Song, C.; Feng, W.; Cai, H.; Xu, D.; Deng, H.; Li, H.; Zheng, D.; Zhu, X.; Wang, H.; Zhu, S. Y.; Scully, M. O. Synthesis of Antisymmetric Spin Exchange Interaction and Chiral Spin Clusters in Superconducting Circuits. *Nat. Phys.* **2019**, *15*, 382-386.
- (4) (a) Kesanli, B.; Lin, W. Chiral Porous Coordination Networks: Rational Design and Applications in Enantioselective Processes. *Coord. Chem. Rev.* **2003**, *246*, 305-326. (b) Barker, J.; Kilner, M. The Coordination Chemistry of the Amidine Ligand. *Coord. Chem. Rev.* **1994**, *133*, 219-300
- (5) (a) Haupt, K.; Linares, A. V.; Bompert, M.; Bui, B. T. Molecular Imprinted Polymers. *Top. Curr. Chem.* **2012**, *325*, 1-28; (b) Lawton, T. J.; Pushkarev, V.; Wei, D.; Lucci, F. R.; Sholl, D. S.; Gellman, A. J.; Sykes, E. C. H. Long Range Chiral Imprinting of Cu (110) by Tartaric Acid. *J. Phys. Chem. C* **2013**, *117*, 22290-22297. (c) Alexander, C.; Davidson, L.; Hayes, W. Imprinted Polymers: Artificial Molecular Recognition Materials with Applications in Synthesis and Catalysis. *Tetrahedron* **2003**, *59*, 2025-2057.
- (6) (a) Patel, R. N. Synthesis of Chiral Pharmaceutical Intermediates by Biocatalysis. *Coord. Chem. Rev.* **2008**, *252*, 659-701. (b) Schmidt, S.; Büchschütz, H. C.; Scherker, C.; Liese, A.; Gröger, H.; Bornscheuer, U. Biocatalytic Access to Chiral Polyesters by An Artificial Enzyme Cascade Synthesis. *ChemCatChem* **2015**, *7*, 3951-3955. (c) Hepworth, L. J.; France, S. P.; Hussain, S.; Both, P.; Turner, N. J.; Flitsch, S. L. Enzyme Cascades in Whole Cells for the Synthesis of Chiral Cyclic Amines. *ACS Catal.* **2017**, *7*, 2920-2925.
- (7) (a) Colacot, T. J. A Concise Update on the Applications of Chiral Ferrocenyl Phosphines in Homogeneous Catalysis Leading to Organic Synthesis. *Chem. Rev.* **2003**, *103*, 3101-3118. (b) Jones, M. D.; Raja, R.; Thomas, J. M.; Johnson, B. F. G.; Lewis, D. W.; Rouzaud, J.; Harris, K. D. M. Enhancing the Enantioselectivity of Novel Homogeneous Organometallic Hydrogenation Catalysts. *Angew. Chem. Int. Ed.* **2003**, *42*, 4326-4331. (c) Lühr, S.; Holz, J.; Börner, A. The Synthesis of Chiral Phosphorus Ligands for use in Homogeneous Metal Catalysis. *ChemCatChem* **2011**, *3*, 1708-1730.
- (8) (a) Müller, C.; Nijkamp, M. G.; Vogt, D. Continuous Homogeneous Catalysis. *Eur. J. Inorg. Chem.* **2005**, *2005*, 4011-4021; (b) Xia, Q. H.; Ge, H. Q.; Ye, C. P.; Liu, Z. M.; Su, K. X. Advances in Homogeneous and Heterogeneous Catalytic Asymmetric Epoxidation. *Chem. Rev.* **2005**, *105*, 1603-1662.
- (9) (a) Savile, C. K.; Janey, J. M.; Mundoff, E. C.; Moore, J. C.; Tam, S.; Jarvis, W. R.; Colbeck, J. C.; Krebber, A.; Fleitz, F. J.; Brands, J.; Davine, P. N.; Huisman, G. W.; Hughes, G. J. Biocatalytic Asymmetric Synthesis of Chiral Amines from Ketones Applied to Sitagliptin Manufacture. *Science* **2010**, *329*, 305-309. (b) Green, A. P.; Turner, N. J.; O'Reilly, E. Chiral Amine Synthesis Using  $\square$ -Transaminases: An Amine Donor that Displaces Equilibria and Enables High-Throughput Screening. *Angew. Chem. Int. Ed.* **2014**, *53*, 10714-10717. (c) Aleku, G. A.; France, S. P.; Man, H.; Sanchez, J. M.; Montgomery, S. L.; Sharma, M.; Leipold, F.; Hussain, S.; Grogan, G.; Tuner, N. J. A Reductive Aminase from *Aspergillus Oryzae*. *Nat. Chem.* **2017**, *9*, 961-969.
- (10) (a) Reetz, M. T. What are the Limitations of Enzymes in Synthetic Organic Chemistry? *Chem. Rec.* **2016**, *16*, 2449-2459. (b) Truppo, M. D. Biocatalysis in the Pharmaceutical Industry: The Need for Speed. *ACS Med. Chem. Lett.* **2017**, *8*, 476-480.
- (11) (a) Vlatakis, G.; Andersson, L. I.; Müller, R.; Mosbach, K. Drug Assay Using Antibody Mimics Made by Molecular Imprinting. *Nature* **1993**, *361*, 645-647; (b) Alexander, C.; Andersson, H. S.; Andersson, L. I.; Ansell, R. J.; Kirsch, N.; Nicholls, L. A.; Mahony, J. O.; Whitecombe, M. J. Molecular Imprinting Science and Technology: a Survey of the Literature for the Years up to and Including 2003. *J. Mol. Recognit.* **2003**, *19*, 106-180. (c) Vasapollo, G.; Sole, R. D.; Mergola, L.; Lazzoi, M. R.; Scardino, A.; Scorrano, S.; Mele, G. Molecularly Imprinted Polymers: Present and Future Prospective. *Int. J. Mol. Sci.* **2011**, *12*, 5908-5945. (d) Verheyen, E.; Schillemans, J. P.; van Wijk, M.; Demeniex, M. A.; Hennink, W. E.; van Nostrum, C. F. Challenges for the Effective Molecular Imprinting of Proteins. *Biomaterials* **2011**, *32*, 3008-3020; (e) Chen, L.; Wang, X.; Lu, W.; Wu, X.; Li, J. Molecular Imprinting: Perspectives and Applications. *Chem. Soc. Rev.* **2016**, *45*, 2137-2211.
- (12) (a) Mondal, P. C.; Fontanesi, C.; Waldeck, D. H.; Naaman, R. Field and Chirality Effects on Electrochemical Charge Transfer Rates: Spin Dependent Electrochemistry. *ACS Nano* **2015**, *9*, 3377-3384; (b) Xiang, S.; Zhang, Y.; Xin, Q.; Li, C. Asymmetric Epoxidation of Allyl Alcohol on Organic-Inorganic Hybrid Chiral Catalysts Grafted onto the Surface of Silica and in the Mesopores of MCM-41. *Angew. Chem. Int. Ed.* **2002**, *41*, 821-824.
- (13) (a) Lee, S. J.; Hu, A.; Lin, W. The First Chiral Organometallic Triangle for Asymmetric Catalysis. *J. Am. Chem. Soc.* **2002**, *124*, 12948-12949. (b) Sinou, D. Asymmetric Organometallic-Catalyzed Reactions in Aqueous Media. *Adv. Synth. Catal.* **2002**, *344*, 211-237.
- (14) (a) Meeuwissen, J.; Reek, J. N. H. Supramolecular Catalysis beyond Enzyme Mimics. *Nat. Chem.* **2010**, *2*, 615-621. (b) Deuss, P. J.; Heeten, R. D.; Lann, W. Kamer, P. C. J. Bioinspired Catalyst Design and Artificial Metalloenzymes. *Chem. Eur. J.* **2011**, *17*, 4680-4698; (c) Luo, M.; Zhang, J. C.; Yin, H.; Wang, C. M.; Morris-Natschke, S.; Lee, K. H. One-Step Templated Synthesis of Chiral Organometallic Salicyloxazoline Complexes. *BCM Chemistry* **2019**, *13*, 1-9.
- (15) (a) Mosbach, K.; Ramström, O. The Emerging Technique of Molecular Imprinting and Its Future Impact on Biotechnology. *Nature Biotechnol.* **1996**, *14*, 163-170; (b) Kulsing, C.; Knob, R.; Macka, M.; Junor, P.; Boysen, R. I.; Hearn, M. T. W. Molecular Imprinted Polymeric Porous Layers in Open Tubular Capillaries for Chiral Separations. *J. Chromatogr. A* **2014**, *1354*, 85-91.
- (16) (a) Masqué, N.; Marcé, R.; Borrull, M. F.; Cormack, P. A. G.; Sherrington, D. C. Synthesis and Evaluation of a Molecularly Imprinted Polymer for Selective On-Line Solid-Phase Extraction of 4-Nitrophenol from Environmental Water. *Anal. Chem.* **2000**, *72*, 4122-4126. (b) Wang, J.; Cormack, P. A. G.; Sherrington, D. C.; Khoshdel, E. Monodisperse, Molecularly Imprinted Polymer Microspheres Prepared by Precipitation Polymerization for Affinity Separation Applications. *Angew. Chem. Int. Ed.* **2003**, *42*, 5336-5338; (c) Saylan, Y.; Yilmaz, F.; Özgür, E.; Derazshamshir, A.; Yavuz, H.; Denizil, A. Molecular imprinting of Macromolecules for Sensor Applications. *Sensors*, **2017**, *17*, 898.
- (17) Chen, L.; Xu, S.; Li, J.; Recent Advances in Molecular Imprinting Technology: Current Status, Challenges and Highlighted Applications. *Chem. Soc. Rev.* **2011**, *40*, 2922-2942.
- (18) Li, Z.; Xu, H.; Wu, D.; Zhang, J.; Liu, X.; Gao, S.; Kong, Y. Electrochemical Chiral Recognition of Tryptophan Isomers

- Based on Nonionic Surfactant-Assisted Molecular Imprinting Sol-Gel Silica. *ACS Appl. Mater.* **2019**, *11*, 2840-2848.
- (19) Liu, X. L.; Tsunega, S.; Ito, T.; Takanashi, M.; Saito, M.; Kaikake, K.; Jin, R. H. Double Chiral Hybrid Materials: Formation of Chiral Phenolic Resin on Polyamine-Associated Chiral Silica. *Chem. Lett.* **2017**, *46*, 1518-1521.
- (20) (a) Hao, C.; Xu, L.; Ma, W.; Wu, X.; Wang, L.; Kuang, H.; Xu, C. Unusual Circularly Polarized Photocatalytic Activity in Nanogapped Gold-Silver Chiroplasmonic Nanostructures. *Adv. Funct. Mater.* **2015**, *25*, 5816-5822. (b) Riva, S. Chirality in Metals: An Asymmetrical Journey Among Advanced Functional Materials. *J. Mater. Sci. Technol.* **2016**, *33*, 795-808. (c) Wattanakit, C. Chiral Metals as Electrodes. *Curr. Opin. Electrochem.* **2017**, *7*, 54-60. (d) Switzer, J. A.; Kothari, H. M.; Poizot, P.; Nakanishi, S.; Bohannon, E. W. Enantiospecific Electrodeposition of a Chiral Catalyst. *Nature* **2003**, *425*, 490-493. (e) Avnir, D. Recent Progress in the Study of Molecularly Doped Metals. *Adv. Mater.* **2018**, *30*, 1706804. (f) Pachón, L. D.; Yosef, I.; Markus, T. Z.; Naaman, R.; Avnir, D.; Rothenberg, G. Chiral Imprinting of Palladium with Cinchona Alkaloids. *Nat. Chem.* **2009**, *1*, 160-164. (g) Kelso, M. V.; Tubbesing, J. Z.; Chen, Q.; Switzer, J. A. Epitaxial Electrodeposition of Chiral Metal Surfaces on Silicon (643). *J. Am. Chem. Soc.* **2018**, *140*, 15812-15819.
- (21) Fang, Y.; Li, C.; Bo, J.; Henzie, J.; Yamauchi, Y.; Asahi, T. Chiral Sensing with Mesoporous Pd@Pt Nanoparticles. *ChemElectrochem* **2017**, *4*, 1832-1835.
- (22) (a) Brubaker, P. E.; Moran, J. P.; Bridbord, K.; Hueter, F. G. Noble Metals: Toxicological Appraisal of Potential New Environmental Contaminants. *Environ Health Perspect.* **1975**, *10*, 39-56. (b) Balcerzak, M. *Encyclopedia of Analytical Chemistry: Applications, Theory and Instrumentation* 2015. (c) Vent, G.; Milne, R. A. Cost Accounting Practices at Precious Metal Mines: A Comparative Study, 1869-1905. *Accounting History* **1997**, *2*, 77-105. (d) Saurat, M.; Bringezu, S. Platinum Group Metal Flows of Europe, Part 1. *J. Ind. Ecol.* **2008**, *12*, 754-767.
- (23) (a) Bullock, R. M.; Abundant Metals Give Precious Hydrogenation Performance. *Science*, **2013**, *342*, 1054-1055. (b) Yang, B.; Burch, R.; Hardacre, C.; Headdock, G.; Hu, P. Origin of the Increase of Activity and Selectivity of Nickel Doped by Au, Ag, and Cu for Acetylene Hydrogenation. *ACS Catal.* **2012**, *2*, 1027-1032.
- (24) (a) Kilgore, U. J.; Robert, J. A. S.; Pool, D. H.; Appel, A. M.; Stewart, M. P.; DuBois, M. R.; Dougherty, W. G.; Kassel, W. S.; Bullock, R. M.; Dubois, D. L.  $[\text{Ni}(\text{P}^{\text{Ph}}_2\text{N}^{\text{C6H4x}})_2]^{2+}$  Complexes as Electrocatalysts for  $\text{H}_2$  Production: Effect of Substituents, Acids and Water on Catalytic Rates. *J. Am. Chem. Soc.* **2011**, *133*, 5861-5872. (b) Bennett, A.; Christie, S.; Keane, M. A.; Peacock, R. D.; Webb, G. The Enantioselective Hydrogenation of Methylacetoacetate over Nickel Catalysts Modified with Tartaric Acid. *Catal. Today* **1991**, *10*, 363-370. (c) Vedenyapin, A. A.; Chankvetadze, B. G.; Klabunavakii, E. I. Studies of Copper-Nickel Catalysts for Enantioselective Hydrogenation. *React. Kinet. Catal.* **1934**, *24*, 77-80. (d) Li, Y. Y.; Yu, S. L.; Shen, W. Y.; Gao, J. X. Iron-, Cobalt-, and Nickel-Catalyzed Asymmetric Transfer Hydrogenation and Asymmetric Hydrogenation of Ketones. *Acc. Chem. Res.* **2015**, *48*, 2587-2598.
- (25) Roche, I.; Chañet, E.; Chatenet, M.; Vondrák, J. Carbon-Supported Manganese Oxide Nanoparticles as Electrocatalysts for the Oxygen Reduction Reaction (ORR) in Alkaline Medium: Physical Characterizations and ORR Mechanism. *J. Phys. Chem. C* **2007**, *111*, 1434-1443.
- (26) (a) Guan, Y. Q.; Han, Z.; Li, X.; You, C.; Tan, X.; Lv, H.; Zhang, X. A Cheap Metal for a Challenging Task: Nickel-Catalyzed Highly Diastereo- and Enantioselective Hydrogenation of Tetrasubstituted Fluorinated Enamides. *Chem. Sci.* **2019**, *10*, 252-256. (b) Shen, X.; Li, Y.; Wen, Z.; Cao, S.; Hou, X.; Gong, L. A Chiral Nickel DBFOX Complex as a Bifunctional Catalyst for Visible-Light-Promoted Asymmetric Photoredox Reactions. *Chem. Sci.* **2018**, *9*, 4562-4568.
- (27) (a) Attard, G. S.; Bartlett, P. N.; Coleman, N. R. B.; Elliott, J. M.; Owen, J. R.; Wang, J. H. Mesoporous Platinum Films from Lyotropic Liquid Crystalline Phases. *Science*, **1997**, *278*, 838-840. (b) Attard, G. S.; Glyde, J. C.; Göltner, C. G. Liquid-Crystalline Phases as Templates for the Synthesis of Mesoporous Silica. *Nature*, **1995**, *378*, 366-368.
- (28) (a) Lee, J.; Kim, J.; Hyeon, T. Recent Progress in the Synthesis of Porous Carbon Materials. *Adv. Mater.* **2006**, *18*, 2073-2094 (b) Ramirez, J. P.; Christensen, C. H.; Egeblad, K.; Christensen, C. H.; Groen, J. C. Hierarchical Zeolites: Enhanced Utilisation of Microporous Crystals in Catalysis by Advances in Materials Design. *Chem. Soc. Rev.* **2008**, *37*, 2530-3542; (c) Reculosa, S.; Heim, M.; Gao, F.; Mano, N.; Ravaine, S.; Kuhn, A. Design of Catalytically Active Cylindrical and Macroporous Gold Microelectrodes. *Adv. Funct. Mater.* **2011**, *21*, 691-698. (d) Xiao, C.; Li, Y.; Lu, X.; Zhao, C. Bifunctional Porous NiFe/NiCo<sub>2</sub>O<sub>4</sub>/Ni Foam Electrodes with Triple Hierarchy and Double Synergies for Efficient Whole Cell Water Splitting. *Adv. Funct. Mater.* **2016**, *26*, 3515-3523. (e) Rouya, E.; Cattarin, S.; Reed, M. L. Kelly, R. G.; Zangari, G. Electrochemical Characterization of the Surface Area of Nanoporous Gold Films. *J. Electrochem. Soc.* **2012**, *159*, K97-K102.
- (29) (a) Yusake, Y.; Tokihiko, Y.; Hitomi, M.; Masato, T.; Tetsuro, S.; Toshiyuki, M.; Tetsuya, O.; Kazuyuki, K. Highly Ordered Mesoporous Ni Particles by Electroless Deposition from Lyotropic Liquid Crystals. *Chem. Lett.* **2004**, *33*, 542-543. (b) Campbell, R.; Bakker, M. G. Electrodeposition of Mesoporous Nickel onto Foamed Metals Using Surfactant and Polymer Templates. *J. Porous Mater.* **2004**, *11*, 63-69. (c) Assavapanumat, S.; Ketkaew, M. Garrigue, P.; Lapeyre, V.; Reculosa, S.; Wattanakit, C.; Kuhn, A. Hierarchical Multiporous Nickel for Oxygen Evolution Reaction in Alkaline Media. *ChemCatChem* **2019**, DOI: 10.1002/cctc.201901509 .
- (30) Nelson, P. A.; Elliott, J. M.; Attard, G. S.; Owen, J. R. Mesoporous Nickel/Nickel Oxide-a Nanoarchitected Electrode. *Chem. Mater.* **2002**, *14*, 524-529.
- (31) (a) Singh, A.; Chang, S. L. Y.; Hocking, R. K.; Bach, U.; Spiccia, L. Highly Active Nickel Oxide Water Oxidation Catalysts Deposited from Molecular Complexes. *Energy Environ. Sci.* **2013**, *6*, 579-586. (b) Zhang, X.; Shi, W.; Zhu, J.; Zhao, W.; Ma, J.; Mhaisalkar, S.; Maria, T. L.; Yang, Y.; Zhang, H.; Hng, H. H.; Yan, Q. Synthesis of Porous NiO Nanocrystals with Controllable Surface Area and their Application as Supercapacitor Electrodes. *Nano. Res.* **2010**, *3*, 643-652.
- (32) (a) May, J. W.; Carroll, C. E. Ionic Monolayers on Metals: II. Neutral Mixed Layers and Surface Reconstruction. *Surface Science* **1972**, *29*, 85-113. (b) Ostyn, K. M.; Carter, C. B. On the Reduction of Nickel Oxide. *Surface Science* **1982**, *121*, 360-374; (c) Alfè, D.; Gironcoli, S.; Baroni, S. The Reconstruction of Nickel and Rhodium (001) Surfaces upon Carbon, Nitrogen or Oxygen Adsorptions. *Surface Science* **1999**, *437*, 18-28.
- (33) (a) Benjamin, J. S. Dispersion Strengthened Superalloys by Mechanical Alloying. *Metallurgical Transactions* **1970**, *1*, 2943-2951. (b) Scorzelli, R. B. A Study of Phase Stability in Invar Fe-Ni Alloys Obtained by Non-Conventional methods. *Hyperfine Interactions*, **1997**, *110*, 143-150. (c) Inoue, A. Stabilization of Metallic Supercooled Liquid and Bulk Amorphous Alloys. *Acta Materialia*, **2000**, *48*, 279-306.

(34) (a) Pedferri, P. Cathodic Protection and Cathodic Prevention. *Construction and Building Materials* **1996**, *10*, 391-402. (b) Bates, J. F. Cathodic Protection to Prevent Crevice Corrosion of Stainless Steels in Halide Media. *Corrosion* **1973**, *29*, 28-32; (c) Mears, R. B.; Brown, R. H. A Theory of Cathodic Protection. *J. Electrochem. Soc.* **1938**, *74*, 519-531.

(35) (a) Chen, B. S.; De Souza, F. Z. R. Enzymatic Synthesis of Enantiopure Alcohols: Current state and Perspectives. *RSC*

*Adv.* **2019**, *9*, 1202-2115. (b) Zheng, Y. G.; Yin, H. H.; Yu, D. F.; Chen, X.; Tang, X. T.; Zhang, X. J.; Xue, Y. P.; Wang, Y. J.; Liu, Z. Q. Recent Advances in Biotechnological Applications of Alcohol Dehydration. *Appl. Microbiol. Biotechnol.* **2017**, *101*, 987-1001.

